N2/CO ratio in comets insensitive to orbital evolution

S. E. Anderson, P. Rousselot, B. Noyelles, E. Jehin, O. Mousis

Monthly Notices of the ROYAL ASTRONOMICAL SOCIETY

MNRAS **524,** 5182–5195 (2023) https://doi.org/10.1093/mnras/stad2092
Advance Access publication 2023 July 13

N_2/CO ratio in comets insensitive to orbital evolution

S. E. Anderson [1,2★] P. Rousselot,[1] B. Noyelles [1] E. Jehin[3] and O. Mousis[2,4]

[1]*Institut UTINAM UMR 6213 / CNRS, Université de Franche-Comté, OSU THETA, BP 1615, 25010 Besançon Cedex, France*
[2]*Aix-Marseille Université, CNRS, CNES, Institut Origines, LAM, 13013 Marseille, France*
[3]*STAR Institute, Université de Liège, Allée du 6 Août 19c, 4000 Liège, Belgium*
[4]*Institut Universitaire de France (IUF), France*

Accepted 2023 July 10. Received 2023 July 10; in original form 2023 March 17

ABSTRACT

Comets are seen as depleted in nitrogen compared to the protosolar value, but a small number exhibit significantly higher than typical N_2/CO ratios: C/1908 R1 (Morehouse), C/1940 R2 (Cunningham), C/1947 S1 (Bester), C/1956 R1 (Arend–Roland), C/1957 P1 (Mrkos), C/1961 R1 (Humason), C/1969 Y1 (Bennett), C/1973 E1 (Kohoutek), C/1975 V1-A (West), C/1986 P1 (Wilson), C/1987 P1 (Bradfield), C/2001 Q4 (NEAT), C/2002 VQ94 (LINEAR), C/2016 R2 (PanSTARRS), and periodic comets 1P/Halley, 29P/Schwassmann–Wachmann 1, and 67P/Churyumov–Gerasimenko. This study examines the composition and dynamical histories of these N_2-'rich' comets to unearth insights into their formation processes. Using updated N_2 fluorescence factors, we re-estimate the N_2/CO ratios of this sample and find that they are consistent with the expected values for comets based on estimations of the protosolar nebula. These also often display larger nucleus sizes and show rapid tail morphology variations due to their ionic nature. Numerical simulations reveal no common dynamical history, suggesting that the N_2/CO ratio is independent of the number of inner Solar System passages and that N_2 is homogeneously distributed within these comets. These volatile-rich comets share an Oort Cloud origin which is consistent with their survival over the past 4.5 Gyr. Our study also suggests that there may be a bias using modern high-resolution spectrometers with narrow slits, which could potentially overlook the ion tail of comets. We advocate for the use of long-slit spectroscopy to potentially detect a wider range of N_2-rich comets, thereby enriching our understanding of comet compositions and origins.

Key words: Comets: general – Comets: individual: C/2016 R2 (PANSTARRS) – protoplanetary discs.

1 INTRODUCTION

Comets are thought to have formed from the agglomeration of icy grains and dust particles leftover from the planetary formation process. As they have been stored at large heliocentric distances, they have undergone little alteration since and thus should represent the composition of the Protoplanetary Disc (PPD) at the location in which they were formed. By investigating the composition of cometary ices undergoing sublimation while a comet approaches the sun we can gain insight into the physicochemical conditions of their formation, thus providing further insight into the nature of the early Solar System at the time and place these comets formed. However, due to the dynamic instability of the early Solar System, these cannot be traced dynamically to their initial formation zone.

Despite comets presenting similar compositions to predicted protosolar abundances, with no depletion of carbon or oxygen, there is a clear deficiency of nitrogen (Geiss 1987). This is evident in the dust of comet 1P/Halley, as the measured elemental N/O abundance is depleted by a factor of 3 with respect to the solar abundance $(N/O)_\odot = 0.13$ (Jessberger & Kissel 1991). The depletion is even stronger when combining measurements of various N-bearing molecules: Wyckoff, Tegler & Engel (1991) estimated that there is a deficiency in the ice component of comet Halley by a factor of 75 with respect to $(N/O)_\odot$ and an overall (dust + ice) elemental nitrogen deficiency of 6. From the detection of a few new N-bearing volatile species, Bockelée-Morvan et al. (2000) inferred a N/O elemental depletion of 15 relative to the solar ratio in the gas phase of comet C/1995 O1 (Hale–Bopp). Since N_2 is the least reactive of all N-bearing species and believed to be the main carrier of nitrogen in the solar nebula, the low abundance of elementary nitrogen must be due to a depletion of N_2 (Feldman, Cochran & Combi 2004). Lodders, Palme & Gail (2009) gave a N_2/CO protosolar nebula value of 0.145 ± 0.048 assuming all the nitrogen was in N_2 and the carbon was in CO. Owen & Bar-Nun (1995) studied the deposition of gases into amorphous water ice in the laboratory and determined that ices incorporated into comets at around 50 K would have N_2/CO $\approx$0.06 if N_2/CO is $\approx$1 in the solar nebula. For comparison, Cochran, Cochran & Barker (2000) found an upper limit for N_2/CO as only 3×10^{-4} for comet 122P/de Vico and 6×10^{-5} for comet Hale–Bopp, which is at least 100× lower than expected. A typical N_2/CO ratio of $<10^{-3}$ is presumed for most comets. This is peculiar considering both Pluto and Triton, which also formed in the outer Solar System, exhibiting N_2-rich surfaces (Cruikshank et al. 1993; Owen et al. 1993; Quirico et al. 1999; Merlin et al. 2018). Mousis et al. (2012) proposed that this could be due to post-accretion internal heating from radiogenic nuclide decay which may explain the absence of nitrogen in comets as N_2 is a poor clathrate former under plausible gas-phase compositions. This would indicate that low temperatures ($\sim$20 K) are needed for pure N_2 condensate formation.

★ E-mail: sarah.anderson@lam.fr

The detection of molecular nitrogen in comets using spectroscopic methods has been challenging as N_2 has no permanent dipole moment, which results in the absence of pure rotational transitions, making the molecule invisible to observations at millimeter-wavelengths. The electronic transitions are only visible in the UV through instruments placed outside of our atmosphere. The presence of N_2 in comet 67P/ Churyumov–Gerasimenko was not detected through any transition but using the ROSINA mass spectrometer *in situ* measurements (Rubin et al. 2015). It is possible to identify N_2 in comets using ground-based telescopes by searching for its daughter-ion, N_2^+, which is detectable in the optical range through the bands of the first negative group ($B^2\Sigma_u^+$ - $X^2\Sigma_g^+$) with the (0,0) bandhead located at 3914 Å. Recently, the long-period comet C/2016 R2 (PanSTARRS) was revealed to be a CO-rich comet (Wierzchos & Womack 2018) and strongly depleted in water, with an H_2^O/CO ratio of 0.0032 (McKay et al. 2019) with an upper limit of < 0.1 (Biver et al. 2018). The spectrum was dominated by bands of CO^+ as well as N_2^+, the latter of which was rarely seen in such abundance in comets (Cochran & McKay 2018; Opitom et al. 2019). It was also found to be C_{2^-}, NH_{2^-}, and CN weak, while being dust-poor (Opitom et al. 2019). This CO-rich and water-poor composition, along with none of the usual neutrals seen in most cometary spectra, makes C/2016 R2 a unique and intriguing object. The observed emission fluxes have been used to calculate ionic ratios of N_2^+/CO^+ in the coma between 0.06 ± 0.01 (Cochran & McKay 2018; Opitom et al. 2019) and 0.08 ± 0.01 (Biver et al. 2018), which would be the same ratio for N_2/CO since ionization efficiencies of N_2 and CO are similar as long as they are fully photodissociated in the coma. Thanks to the UVES high-resolution spectra obtained of the comet (Opitom et al. 2019), we were able to produce a new fluorescence model of N_2^+ and calculate a more precise g-factor or fluorescence factor of $g = 4.90 \times 10^{-2}$ photons.s^{-1}.molecule^{-1}for the entire band (Rousselot et al. 2022). We calculated a production rate of $Q(N_2)$ $\sim 10^{28}$ molecules.s^{-1}, which, when compared to the production rate of Q(CO) $\sim 1.1 \times 10^{29}$ molecules.s^{-1} (Cochran & McKay 2018), gives an N_2/CO ratio of 0.09, which is consistent with previous determinations of intensity ratios in the PSN. This is one of the highest of such ratios observed for any comet so far (Anderson et al. 2022a) and in line with the predictions of Owen & Bar-Nun (1995) and (Lodders et al. 2009). This is larger than what was measured for comet 67P with the *in situ* ROSINA mass spectrometer, with an N_2/CO ratio of 0.0287 (Rubin et al. 2020), obtained much closer to the nucleus.

In this paper, we intend to review the links between N_2-rich comets in the hopes of finding shared characteristics that could point to their formation conditions. We consider a comet N_2-rich if their N_2/CO ratio exceeds 0.01, as a typical cometary N_2/CO ratio is in the order of $>10^{-3}$ if any is detected at all (Cochran et al. 2000; Cochran & Cochran 2002). We begin by exploring the literature in order to find N_2-rich comet observations and attempt to identify similarities in Section 2 before re-estimating their N_2/CO ratios using the new fluorescence factors from Rousselot et al. (2022) in Section 3. We then examine their recent dynamical history using numerical simulators in search of a dynamical link in Section 4. We consider the similarities of these objects with known N_2-rich objects in our Solar System, Pluto and Triton, in Section 5 before discussing these results in Section 6.

2 COMPARISON OF COMETS IN OUR SAMPLE

The only instances of N_2^+ being detected in high quantities comets were in C/1908 R1 (Morehouse) (de La Baume Pluvinel & Baldet 1911), C/1947 S1 (Bester) (Swings & Page 1950), C/1961 R1 (Humason) (Greenstein 1962), 1P/Halley (Wyckoff & Theobald 1989; Lutz, Womack & Wagner 1993), C/1987 P1 (Bradfield) (Lutz et al. 1993), 29P/Schwassmann–Wachmann 1 (Korsun, Ivanova & Afanasiev 2008; Ivanova et al. 2016, 2018), and C/2002 VQ94 (LINEAR) (Korsun et al. 2008; Korsun et al. 2014). These comets repeatedly are cited as examples of exceptions to the rule of N_2-depletion in comets. We also expand our sample by including those from table III of Cochran et al. (2000): C/1940 R2 (Cunningham), C/1956 R1 (Arend–Roland), C/1957 P1 (Mrkos), C/1969 Y1 (Bennett), C/1973 E1 (Kohoutek), C/1975 V1-A (West), and C/1986 P1 (Wilson). Their N_2/CO ratios were calculated in conjunction with the authors' personal communication with Claude Arpigny and their N_2^+/CO^+ ratios were adapted to use the CO^+(2,0) bands. C/1969 T1 (Tago-Sato-Kosaka) was also included on their list, but only measured for an upper limit of 0.03, and there is no current evidence of a rich N_2 composition. Similarly, we expand our list with C/2001 Q4 (NEAT) (Feldman 2015), which was determined using FUSE observations. It should be noted that neither N_2^+ nor CO^+ were detected with UVES in C/2001 Q4 (NEAT). However, this might be evidence of an example of observational bias when the high-resolution spectrograph is centered on the nucleus. Meanwhile, C/2016 R2 has provided us with the highest resolution spectra of N_2^+ observed in comets to date (Cochran & McKay 2018; Wierzchos & Womack 2018; McKay et al. 2019; Opitom et al. 2019).

We begin by investigating the immediate similarities between the comets of our sample. We present their orbital elements and volatile composition in Table 1 while the eccentricity as a function of perihelion distance is shown in Fig. 1. All values of the orbital elements are retrieved from the JPL Small Body Data base (SBD) Lookup tool. The immediate link between the non-periodic comets is that they are all quasi-parabolic, with high eccentricities nearing or superior to 1. We will investigate the dynamical history of these objects in Section 4.1. However, the *in situ* detection of N_2 in comet 67P by Rubin et al. (2020), along with elevated N_2/CO ratios in comets 1P and 29P make us wonder how the periodic comets fit into this puzzle. 1P is a Halley-type comet, 67P is a Jupiter Family comet (JFC), and 29P is a Centaur, highlighting the diversity of these objects. The discrepancy between the detection of N_2 in the nucleus of comet 67P by *in situ* Rosina mass spectrometer measurements and the lack of its detection from ground-based telescopes in the coma raises an interesting question. Further research and observational studies are needed to better understand the mechanisms governing the release and visibility of N_2 (and ions in general) in cometary comas, as well as the specific properties of individual comets that may influence the presence or absence of N_2^+ in their comae. It is possible N_2 could be found in many other comets if we were to directly measure near their surfaces, but more *in situ* probes are required. As a result, 67P is difficult to place in our study.

2.1 Nucleus size

Based on the nucleus magnitude provided by the ephemeris and a realistic geometric albedo of about 0.04, we can estimate effective radii (R_n) of our sample comets from their absolute nuclear magnitude using the standard methodology devised by Russell (1916) and reformulated by Lamy et al. (2004):

$$R_n = \frac{1.496 \times 10^{11}}{\sqrt{p}} 10^{0.2(m_\odot - H)}, \quad (1)$$

where R_n is the comet's nucleus in meters, p is the geometric albedo, $m_\odot$ the apparent magnitude of the sun, and H the absolute magnitude of the comet's nucleus (i.e. the magnitude at $r_h = \Delta = 1$ au,

Table 1. Orbital elements along with H_2O/CO and N_2/CO abundance ratios of comets with peculiar N_2-rich and/or H_2O-poor compositions. Diameters determined based on the nucleus magnitude are marked with an asterisk (∗).

Comet	P (yr)	q (au)	e	i (deg°)	D (km)	H_2O/CO	N_2/CO
C/1908 R1 (Morehouse)	–	0.945	1.0009	140.17	–	–	≥0.06[a]
C/1940 R2 (Cunningham)	–	0.368	1.0005	49.89	–	–	≥0.04[a]
C/1947 S1 (Bester)	–	0.748	1.0003	140.56	37∗	–	0.05–0.09[a]
C/1956 R1 (Arend–Roland)	–	0.316	1.0002	119.94	–	–	>0.09[a]
C/1957 P1 (Mrkos)	12 415	0.355	0.9992	93.96	24∗	–	0.02[a]
C/1961 R1 (Humason)	2944	2.133	0.9896	153.28	30–41	5[b]	0.02–0.03[a]
C/1969 T1 (Tago-Sato-Kosaka)	512 287	0.472	0.9999	75.82	–	–	≤0.03[a]
C/1969 Y1 (Bennett)	1747	0.538	0.9962	90.04	–	–	0.03[a]
C/1973 E1 (Kohoutek)	–	0.142	1.0000	14.30	–	–	0.07[a]
C/1975 V1-A (West)	–	0.197	1.0000	43.07	–	–	0.008[a]
C/1986 P1 (Wilson)	–	1.199	1.0003	147.12	33∗	–	0.07[a]
C/1987 P1 (Bradfield)	2122	0.869	1.0000	34.09	–	–	0.02 ± 0.07[c]
C/2001 Q4 (NEAT)	–	0.962	1.0007	99.64	–	13.88[d]	< 0.03[d]
C/2002 VQ94 (LINEAR)	2863	6.797	0.9663	70.52	96 ± 4[e]	–	0.06[e]
C/2016 R2 (PanSTARRS)	18 709	2.602	0.9963	58.22	38	<0.0032[f]	0.06 ± 0.01[g]
1P/Halley	76	0.586	0.9671	162	11	–	0.005[h]
29P/Schwassmann–Wachmann 1	14.6	5.734	0.0440	9.37	60.4[i]	0.22[j]	0.01[k]
67P/Churyumov–Gerasimenko	6.43	1.243	0.6497	3.87	4	32.25[l]	0.03[l]
122P/de Vico	74.35	0.659	0.9627	85.38	–	–	$<3 \times 10^{-4}$ m
153P/Ikeya–Zhang	365.50	0.507	0.9901	28.12	–	–	$<5.4 \times 10^{-4}$ m
C/1995 O1 (Hale–Bopp)	2363.53	0.891	0.9950	89.29	60 ± 20[n]	∼1[o]	$<6.5 - <9.9 \times 10^{-5}$ m

Notes. [a] Values from Table III of Cochran et al. (2000) based on their personal communication with C. Arpigny and photographic plates, save for C/1973 E1 (Fourier Transform spectrometer) and C/1986 P1 (CCD).
[b] Estimated from Greenstein (1962) & Arpigny (1964).
[c] Lutz et al. (1993).
[d] Feldman (2015) from the N_2(0,0) band of the ($c_4'^1\Sigma_u^+ - X^1\Sigma_g^+$) system at 958 Å.
[e] Korsun et al. (2014).
[f] McKay et al. (2019).
[g] Opitom et al. (2019).
[h] Wyckoff et al. (1991): CO/N_2 ∼ 200.
[i] Schambeau et al. (2015).
[j] Ootsubo et al. (2012).
[k] Ivanova et al. (2016).
[l] Rubin et al. (2015, 2020).
[m] Cochran et al. (2000); Bar-Nun, Notesco & Owen (2007).
[n] Fernández (2002).
[o] Womack et al. (2021).

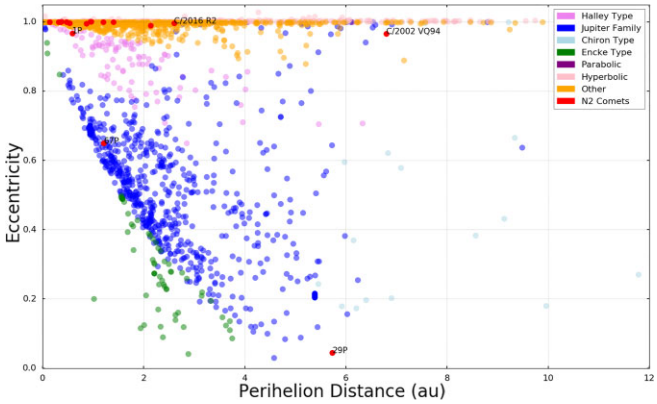

Figure 1. Eccentricity as a function of perihelion for all known comets (elements retrieved from the *JPL Small-Body Data base Lookup (SBD)*) with the comets of our sample in red. Almost all N_2-rich comets in our sample are quasi-parabolic.

$\alpha = 0°$), where α represents the phase angle (angle made between the Earth-comet-sun). We take −26.93 for the r-band magnitude of the sun (Colina, Bohlin & Castelli 1996), and 11.2 for the absolute magnitude of the comet nucleus from the SBD. Comet sizes we have estimated based on the nucleus's absolute magnitude are marked with an asterisk (∗). The resulting nucleus diameters are shown in Fig. 2, along with all other known comet nuclei. The nearly isotropic comets of our study with measurable nucleus size appear to have larger than common nucleus size, with the smallest being C/1957 P1 (Mrkos) at ∼24 km in diameter followed by C/2016 R2 and C/1961 R1 with a ∼35 km diameter. The largest are comet 29P with a confirmed 60.4 km diameter (Schambeau et al. 2015) and comet C/2002 VQ94 with an anticipated 96 km diameter (Korsun et al. 2014). If this were the entirety of our sample size, then we could say these are large, long-period comets originating from the distant Oort cloud. Seeing their volatile-rich composition, they should be dynamically new, and perhaps represent some of the oldest comets available to us, offering us a pristine look at the early Solar System. comet 29P may be a Centaur, but it is also exceptionally large, with a nucleus estimated at 60.4 km in diameter (Schambeau et al. 2015). With such a high volatile content, it must have been preserved at a high

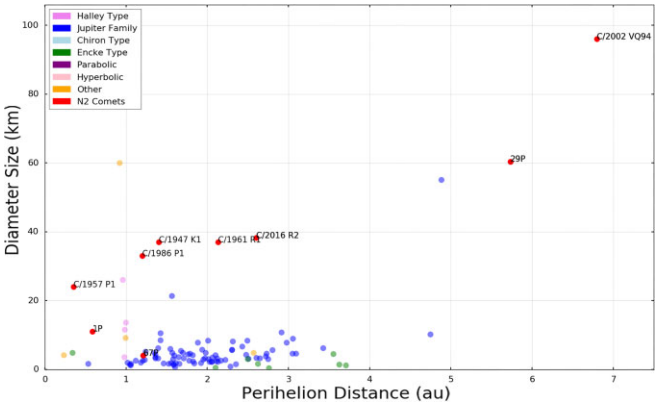

Figure 2. Estimated diameters of all comets in our study (red) compared to all known comet nucleus diameters as a function of perihelion distance. The comets within our sample are larger than typical. 67P is within the average range of nucleus diameters, but the N_2 was measured *in situ* using the Rosina mass spectrometer.

heliocentric distance until its recent capture. Visual observations also seem to indicate that these comets are active at higher heliocentric distances and have rapidly changing tail morphology. Indeed, 29P has a perihelion of 5.7 au, and has been active since its discovery (Schambeau et al. 2015). However, some of the comets in our sample present an opposing view: Hale–Bopp, despite being the same size as 29P (Fernández 2002), has a very low N_2/CO ratio: thus, size is not the defining factor of a N_2-rich comet and this ratio is not linked directly to nucleus size.

There appears to be a cluster of N_2-rich comets with high-eccentricities and a perihelion between 0.7 and 1 au, with 1P/Halley just outside this cluster. The only N_2-rich comets we have observed with a perihelion >3 au are also the largest in our study. At first glance, this would seem natural: despite outgassing at large heliocentric distances, we would miss small comets with large q due to the limitations of our observational technology. Large cometary nuclei produce brighter comets than small cometary nuclei and are thus easier to detect, and since the amount of gas and dust emitted by a comet varies as a function of the heliocentric distance, its perihelion distance plays a key role in its discoverability. However, many of these small q comets are seen on approach at much larger heliocentric distances than the q of these large comets; we should also be observing many more massive volatile-rich comets with small q, especially if they are such powerful outgassers. It is strange that mega-comets do not seem to reach low perihelion. It is possible that comets of this size would not survive such a close approach to the sun. In a study of 105 short-period comets (here, P<20 yr) with known nuclei radii, Hughes (2003) found that a value of $q \simeq 2.7$ au divides the comets into an outer Solar System group which is hardly affected by decay and an inner Solar System group which are decaying quickly. This distance separates comets that have negligible water sublimation from comets that are decaying speedily. This is interesting, as the cluster of N_2-rich comets has a q <2.7 au. It would be interesting to see how this relates to the position of the water-iceline.

It is important to approach the measurements of nucleus size in comets with caution, as these values are derived from ground-based observations of nucleus magnitude. The presence of high volatile content in these comets could potentially impact the magnitude, as Russell (1916) and Lamy et al. (2004)'s estimation was established based on water-rich comets. Biver et al. (2018) estimated that the outgassing rate of C/2016 R2 could be supplied by a pure CO ice object of only 3 km in diameter. Thorough thermal and structural modelling based on possible compositions is essential in order to determine if we are correctly estimating nucleus sizes.

2.2 Dust composition

The $Af\rho$ parameter serves as a proxy for dust production, with a value of 1000 cm corresponding to a dust production rate of approximately 1 ton s^{-1} (A'Hearn et al. 1984, 1995). This parameter is proportional to the dust loss rate multiplied by the dust particles' cross-section within the aperture. C/2016 R2 exhibited a lack of a dust tail (Biver et al. 2018; Cochran & McKay 2018), suggesting low dust production. Previous studies reported $Af\rho$ values ranging from 530 to 830 cm (Noël 2018), with an average of 670 cm, indicating relatively lower dust production compared to gaseous production. In the case of C/2016 R2, utilizing observations from the TRAPPIST telescopes, a $\log [Af\rho/Q(CN)] = -21.78 \pm 0.14$ was derived Opitom et al. (2019). Despite its faint CN emission, the observed $Af\rho$ value falls within the range, suggesting C/2016 R2 is dust-poor and possibly associated with a differentiated object.

In contrast, comet C/1956 R1 (Arend–Roland) exhibited a dust-rich composition, as well as a high N_2 content. At perihelion, the comet was emitting an estimated 7.5×10^4 kg s^{-1} of dust and was releasing roughly 1.5×10^{30} gas molecules s^{-1} as calculated by Finson & Probstein (1968). These findings suggest that the low dust content observed in C/2016 R2 is not necessarily linked to its volatile content. Further investigations into the dust composition of more H_2O-poor comets would provide insights into any potential connections. However, since these comets are so rare, we may need to wait for quite some time.

2.3 Historic observations of N_2^+

Three comets which were often cited as having N_2-rich compositions pre-High-Resolution spectrographs were C/1908 R1 (Morehouse) (de La Baume Pluvinel & Baldet 1911), C/1947 S1 (Bester) (Swings & Page 1950), and C/1961 R1 (Humason) (Greenstein 1962). While their observation was done through the use of photographic plates, and the colour was not visible to the naked eye, the intensity of their spectra convinced astronomers that they were bluish in nature. Glancy (1909) mentions that while comet Daniel 1907 (another vibrant comet at the time) was visually brighter, comet Morehouse 'photographed more readily', and the images were located in the blue, violet, and ultraviolet, due to stronger emissions in the blue and violet 'photographic regions.' It was 'consequently blue' and even to the naked eye had a 'bluish sheen' (Guillaume 1908). This is similar to C/2016 R2, which was bright blue due to its CO^+ ionic tail composition (Opitom et al. 2019).[1]

Most comets in our sample were described as having rapid variations in morphology: Comet C/1908 R1 repeatedly lost its tail and formed new ones; at times, the tail seemed to split into up to six or eight separate tails, depending on the source (Chambers 1909) and it cycled through active and inactive phases (Christie 1908). Comet C/1961 R1 had an unusually disrupted or 'turbulent' appearance (Brandt & Chapman 2004): At one point, between two observations in July 1962, the tail broke off the nucleus (van Biesbroeck 1962). Comet C/1987 P1 (Bradfield) presented 'impressive temporal variability' (Lutz et al. 1993) and had two observed events of plasma tail separation, on 1987 October 19–20th (Cimati 1989), and 1987

[1] https://www.eso.org/public/images/potw1940a/

December 20 (Cremonese & Fulle 1988). These 'early' comets had tails that were considered 'tremendously active' (Swings 1965). These comets, C/1908 R1, C/1961 R1, C/1987 P1, and C/2016 R2 were also observed to be blue, which is a result of bright CO^+ lines. 29P frequently undergoes massive outbursts ($\sim$7 yr^{-1}) which cause the coma to brighten by 1–5 magnitudes, which were even suggested to be caused by seasonal cryovolcanic activity (Miles 2016).

Observations of these comets also note that CN is in low quantities or entirely missing. This is noted for comets C/1908 R1 de La Baume Pluvinel & Baldet (1911), C/1961 R1 (present but weaker than expected) (Warner & Harding 1963), C/1987 (Lutz et al. 1993), and C/2016 R2 (Opitom et al. 2019).

2.4 Historical observational bias

When reading the literature, it became evident that the N_2 depletion in comets is a more recent discovery, and that comets were believed to be N_2 rich until the 1908's. This was due to an observational bias: when Count Aymar de la Baume Pluvinel adapted the technology to the use of objective prisms to observe comets, the long exposures more readily captured comet nuclei, while the tails were bright enough to be photographed on plates. The first comet to have its tail photographed was C/1907 L2 (Daniel), in which he found massive amounts of CO^+ in the tail, followed by the spectacular C/1908 R1 (Morehouse), which has a tail that proved to be rich in CO^+ and N_2^+. Comet C/1947 S1 (Bester) provided the first real look into comet tails using modern spectroscopy: CO^+ bands were once again identified, and N_2^+, 'as expected' (Swings 1965), and it was the first time CO_2^+ emission was identified in the optical spectrum of a comet. Astronomy textbooks at the time described comet tails to be both CO^+ and N_2^+ rich, 'as is well known' and these were 'the two characteristic molecules of the comet-tail spectra' (Swings & Page 1950). Since the method of obtaining cometary spectra using objective prisms was used until the 1940s, the only spectra of tails obtained before 1940 were of C/1908 R1 (Morehouse), and C/1911 O1 (Brooks), which also had a CO^+ tail, comet tails were thought to have this ionic composition until the mid XX^{th} century. It was only when applying these spectroscopy techniques to comets using their modern technology that they discovered this was an outlier, not the rule: these ionic tails were incredibly bright, thus enabling spectroscopic measurements to be taken, creating an observational bias. Comet tails were thus thought to be rich in N_2^+ until the N_2 depletion became more apparent in the 1960s and 1970s thanks to more powerful spectroscopes. The N_2 depletion was cemented by the 1985 flyby of Halley's comet by the *Giotto* spacecraft (Geiss 1987). Lutz et al. (1993) says that N_2^+ is 'rarely reported' in cometary plasma. It would appear the observational bias of bright N_2^+-rich tails being easier to study with spectroscopy before the use of high spectral and geometrical resolution led to the prevalence of this belief.

3 RE-ESTIMATION OF THE N_2/CO RATIO

As N_2 was previously unidentified – or in such small quantities as to be seen as little to no importance – no fluorescence model of N_2^+ had yet been made. In order to estimate the quantity of N_2 until now, we have relied on abundance ratios with other, already quantified, components. In most cases, an estimate of the quantity of N_2 was made through the abundance ratio with CO. Since the column density of a species is given as

$$N = \frac{I_{v'v''}}{g_{v'v''}},$$

where N is the column density, $I_{v'v''}$ the integrated band intensity, and $g_{v'v''}$ the excitation factor, we can determine the ratio of column density for these two species to be

$$\frac{N_2^+}{CO^+} = \frac{g_{CO^+}}{g_{N_2^+}} \frac{I_{N_2^+}}{I_{CO^+}}. \quad (2)$$

This gives us our first estimate of the quantity of N_2^+ present in the comets of our sample. By measuring the band intensity of the observed N_2^+ in cometary spectra, assuming that solar resonance fluorescence is the only excitation source, the observed emission fluxes have been used to calculate ionic ratios of N_2^+/CO^+ in the coma. This would be the same ratio for N_2/CO since N_2 and CO should be released in the same proportion as they exist in the ices because their photoionization rates are similar (Bar-Nun, Kleinfeld & Kochavi 1988; Huebner, Keady & Lyon 1992). CO could be produced by the dissociation of CO_2: in that case, we would expect to see CO_2^+ in C/2016 R2's spectra, but the CO_2^+/CO^+ was only 1.1. CO and N_2 should then be ionized in proportion to the amount of neutrals and $N_2/CO = N_2^+/CO^+$ in the coma. While the ratio of species seen in the gas phase is not necessarily representative of the ratio of the ices in the nucleus, neither CO nor N_2 are terribly reactive with other species. Chemical reactions probably would not alter this ratio much, and the ratio is not expected to change with heliocentric distance. However, previous studies have highlighted the presence of a rich CO chemistry in comets (Pierce & A'Hearn 2010; Raghuram & Bhardwaj 2012), suggesting that CO abundances may experience modest changes on the order of 10 per cent due to photochemical processes. Although our conclusions remain unaffected by these potential changes, this is worth consideration.

In the past, the value of $g_{N_2^+}$ used for the $N_2^+(0, 0)$ band has been $g(0, 0) = 7 \times 10^{-2}$ photon s^{-1} ion^{-1} for 1 au. For consistency, this is compared to the fluorescence efficiency of the $CO^+(2, 0)$ band, with a $g(2, 0)$ of $g = 3.52 \times 10^{-2}$ photons s^{-1} $molecule^{-1}$ at 1 au provided by Magnani & A'Hearn (1986). Thanks to the quality of the spectra from the bright emission of comet C/2016 R2's N_2^+, we were able to improve the value of $g_{N_2^+}$, finding g of $g = 4.90 \times 10^{-2}$ photons s^{-1} $molecule^{-1}$ for the $N_2^+(0, 0)$ band at 1 au (Rousselot et al. 2022). The relationship between the two fluorescence factors is a straightforward ratio, as shown in equation (2), allowing for easy replacement of the old value of $g_{N_2^+}$ with the newly calculated value. The updated results are presented in Table 2. The fluorescence factor has been scaled with the square of the heliocentric distance based on modelling at different distances (see table 1 of Rousselot et al. (2022)), providing a highly accurate approximation for the range of heliocentric distances examined in this study. We see that the newly estimated N_2/CO ratios are much closer to the expected value of 0.145 calculated by Lodders et al. (2009), as shown in Fig. 3. It would appear that the comets in our sample have a composition consistent with the protosolar nebula. What is strange is that their composition should thus be that of a 'typical' comet, yet they are only a small minority of comets we have observed.

Unfortunately, most of the comets in our sample were observed using photographic plates. These had much lower efficiency than our current CCD detectors, and as a result these original observations of cometary spectra were obtained with lower resolution. It would appear comet C/2016 R2 and comet C/2002 VQ94 (LINEAR) present identical N_2/CO ratios, and both are examples of recent comets observed with high-resolution spectroscopy with obvious strong bands of N_2^+. C/2002 VQ94 was first detected at $r_h = 10.02$ au (Tichy et al. 2002) and may be one of the largest comets ever observed, with

Table 2. Updated N_2/CO ratios for all comets with a known N_2 composition.

Comet designation	Old N_2/CO	Updated N_2/CO	Reference
C/1908 R1 (Morehouse)	≥0.06	≥0.085	Cochran et al. (2000)
C/1940 R2 (Cunningham)	≥0.04	≥0.057	Cochran et al. (2000)
C/1947 S1 (Bester)	0.05–0.09	0.071–0.125	Cochran et al. (2000)
C/1956 R1 (Arend–Roland)	>0.09	>0.125	Cochran et al. (2000)
C/1957 R1 (Mrkos)	0.02	0.028	Cochran et al. (2000)
C/1961 R1 (Humason)	0.02–0.03	0.028–0.043	Cochran et al. (2000)
C/1969 T1 (Tago-Sato-Kosaka)	≤0.03	≤0.043	Cochran et al. (2000)
C/1969 Y1 (Benett)	0.03	0.043	Cochran et al. (2000)
C/1973 E1 (Kohoutek)	0.07	0.100	Cochran et al. (2000)
C/1975 V1-A (West)	0.008	0.011	Cochran et al. (2000)
C/1986 P1 (Wilson)	0.07	0.100	Cochran et al. (2000)
C/1987 P1 (Bradfield)	0.02	0.028	Lutz et al. (1993)
C/2001 Q4 (NEAT)	<0.03	<0.043	Feldman (2015)
C/2002 VQ94 (LINEAR)	0.06	0.085	Korsun et al. (2014)
C/2016 R2 (PanSTARRS)	0.06	0.089	Opitom et al. (2019)
1P/Halley	0.005	0.007	Wyckoff et al. (1991)
29P/Schwassmann–Wachmann 1	0.01	0.014	Ivanova et al. (2016)
122P/de Vico	3×10^{-4}	4.2×10^{-4}	Cochran et al. (2000)
153P/Ikeya–Zhang	$<5.4 \times 10^{-4}$	$<7.5 \times 10^{-4}$	Bar-Nun et al. (2007)
C/1995 O1 (Hale–Bopp)	$<6.5 \times 10^{-5} - <9.9 \times 10^{-5}$	$<9.2 \times 10^{-5} - <1.4 \times 10^{-4}$	Cochran et al. (2000)

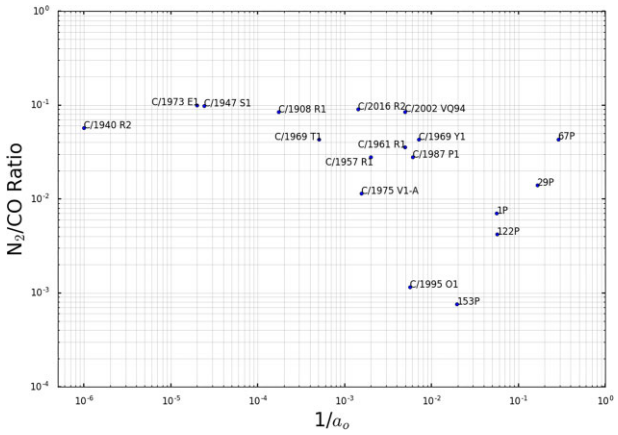

Figure 3. Re-estimated N_2/CO ratio of all comets for which N_2 was identified as a function of the inverse of their semimajor axis, $1/a_0$. There is a seemingly linear relationship between the periodic comets, which does not exist for the nearly isotopic comets in our sample. However, due to the small sample size, this may not be indicative.

a nucleus estimated to be ∼100 km in diameter (Korsun et al. 2014). The cometary activity was first detected at the end of August 2003 when the comet was at $r_h = 8.36$ au. This was the first time these ionic emissions had been observed in such great quantities, and at such a large heliocentric distance. Ivanova et al. (2016) measured N_2^+/CO^+ as 0.013 for comet 29P/Schwassmann–Wachmann 1 at 5.25 au, but the N_2^+ feature is not well defined in these low-resolution spectra.

4 DYNAMICAL FAMILIES

4.1 Numerical simulations

Despite the high precision of modern telescopes, our knowledge of the orbital elements still contains uncertainties: our observation arcs are short, due to the limited amount of time the comet is visible. These remain quite small but can have a great impact on the dynamical evolution of comets. In order to take these uncertainties into account, we compute the dynamical evolution not only of the comet but also of its 'clones', massless facsimiles with orbital elements generated within these uncertainties. These are potential alternative initial conditions for the comet we wish to study. The resulting dynamical history will then be evaluated based on the dispersion of these clones, which provides a statistical model of the potential histories. We take the orbital elements provided by the *JPL Small Body Data base* along with the orbital covariance matrix. We then generate 1000 clones using a multivariate normal distribution with the object's orbital elements as the mean.

4.1.1 Dynamical history of C/2016 R2 (Panstarrs)

In order to estimate the dynamical history of C/2016 R2, we selected two independent dynamical models:

(i) Model 1: we simulate the orbit of C/2016 R2 perturbed by the eight planets using `MERCURY`, a general-purpose software package for carrying out *N*-body orbital integrations for problems in Solar System dynamics Chambers (1999, 2012), chosen for its processing speed. We select its `Hybrid` integration algorithm. We use the Osculating Orbital Elements on Epoch 2458267.5 (2018-May-29.0) as the mean, solution date: 2019-April-15 23:33:5 (Reference: JPL 43, heliocentric IAU76/J2000 ecliptic) provided by the JPL *Small Body Data base* (SBD). At the time we did our simulations, the non-gravitational forces were unknown: now, both A1 and A2 are available on the SBD. `REBOUND` will use these automatically.

(ii) Model 2: we simulate the orbit of C/2016 R2 perturbed by the eight planets with `REBOUND`, a commonly used *N*-body integrator, popular for its simple interface and efficient integrators (Rein & Liu 2012). We select the high accuracy non-symplectic integrator with adaptive timestepping (IAS15). `REBOUND` will automatically download the orbital elements of the bodies from the JPL *Horizons* data base (JPL 43 (heliocentric IAU76/J2000 ecliptic)) for the date 2018-May-29.0.

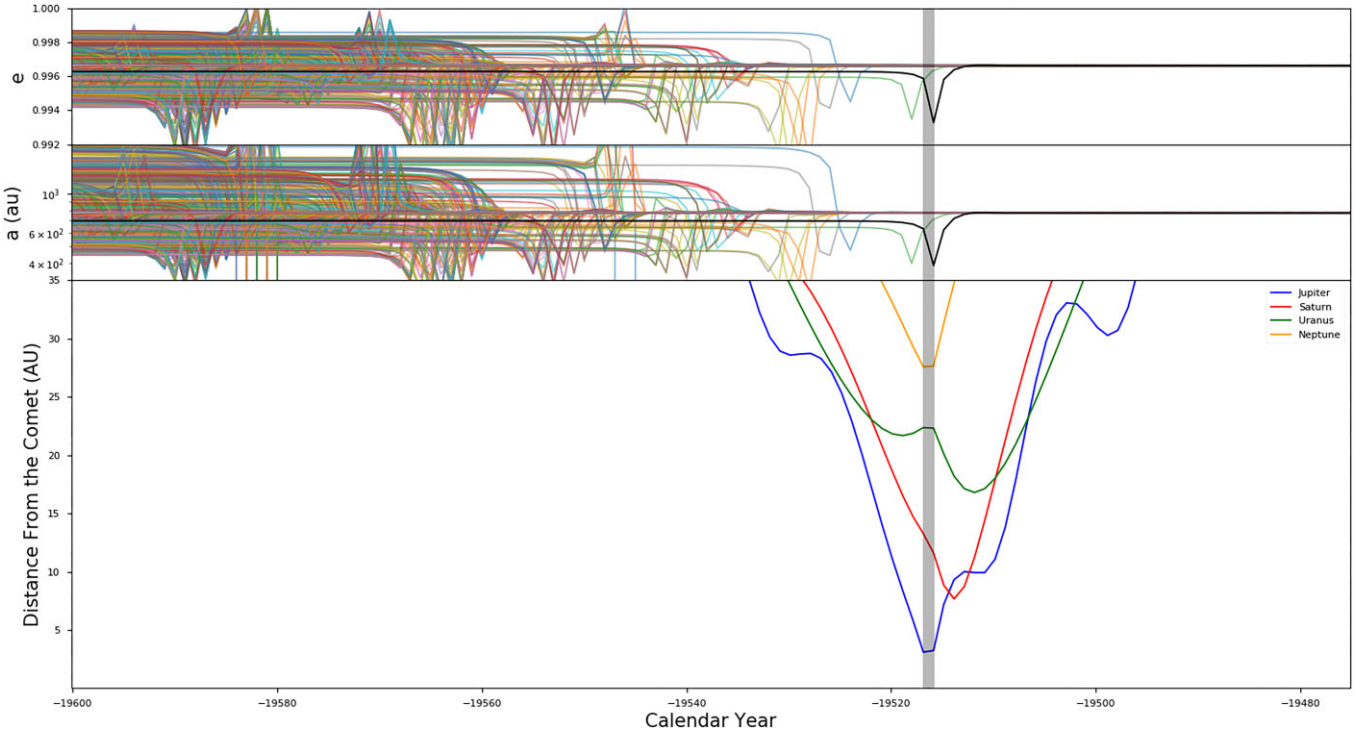

Figure 4. The dynamical history of C/2016 R2 (black) and its 1000 clones (colours), from our second model, with REBOUND shown at the moment of their close encounter with the giant planets. The shaded section corresponds to the moment the close encounter is likely to have occurred. This scatters the clones and renders a further evaluation of its dynamical history past this point futile.

For both models, the planets' initial orbits are also generated on this date from the JPL Horizons data base. As the simulation advances in time, the positions of the eight planets and each C/2016 R2 clone are calculated at each time-step. The clones are seen as independent test particles and do not interact with each other. We run the integration over 1 Myr in negative time.

For Model 1, the clones do not converge towards a single result: the final clones are split almost in half, with 43 per cent of clones ending the simulation with $e > 1$ and 53 per cent with $e < 1$. We also lose 45 clones (>5 per cent) during the simulation, due to how MERCURY handles collisions with the larger planets. The clones share the same trajectory for a single orbit, or $\sim$ 19 000 yr, at which point C/2016 R2 is subjected to close encounters with the giant planets, where the clones passed on average 1.1 au from Jupiter. For such a small object, massless in our simulations, even approaching <2 au of the giant planets will affect the trajectory greatly. This past close encounter is very sensitive to the initial conditions, and with the small variations in our clones, they are scattered on many possible orbits. Each time a comet crosses the orbit of a giant planet, it receives a small 'kick' causing its eccentricity and semimajor axes to increase, while the perihelion distance remains constant. Once the eccentricity of a small body is $e \geq 0.998$ and its semimajor axis is $\geq$ 20 000 au, the galactic tidal field starts to dominate. As soon as the perihelion distance exceeds the semimajor axis of the giant planet $q > a_P$, the eccentricity of the planetesimal's orbit continues to be reduced until the galaxy starts damping its eccentricity and randomizing the inclination. In this case, the object would be considered bound to the sun and part of the Oort cloud. Its final orbit entirely depends on the last interaction it had with a giant planet. What is clear is that we cannot quantify when the last interaction occurred, as each successive interaction erases the memory of the last one. For this reason, it is impossible to determine the trajectory of a comet with any close encounter in its dynamical past and our knowledge of C/2016 R2's past is only certain for this 19 000-yr window: beyond this, its behaviour is chaotic.

As a result, we limit our integration time for Model 2. We see that the same close encounter occurs, and we can not improve the dynamical history by changing integrators. We see the result of the close encounter with the giant planets in Fig. 4. The uncertainties on the comet's ephemeris combined with the limitations of our numerical integrators mean that we will never see C/2016 R2's history before this close encounter. The integration is thus stopped at 25 kyr to avoid wasting computing time. At this point, the nature of the comet is already a 50–50 split of fully hyperbolic or nearly hyperbolic. This is a common issue with comet dynamics.

We also investigated the possibility that C/2016 R2 could have resulted from a recent collision in the outer Solar System. In the case of collisional asteroid families, the orbital elements are similar. Unfortunately, none of our N_2-rich comets share enough orbital elements to have come from a unique object. We could assume that C/2016 R2 was created via impact with a local TNO. We simulated the trajectory of 1000 clones over 15 000 yr and looked for possible close encounters with the 17 largest TNOs (Eris, Gonggong, Haumea, Makemake, Pluto, Quaoar, Sedna, 2002 MS4, Orcus, Salacia, 2014 EZ51, 2002 AW197, 2013 FY27, 2010 JO179, 2003 AZ84, Varda, and 1995 SM55) with over 700 km in diameter. We found the percentage of 'close' encounters to be so small that it would most likely be insignificant (> 1 per cent) which allows us to rule out any impacts in its recent history. While it's equally possible that a collision occurred much longer ago, our clones disperse too quickly to have any chance of tracking their path back reliably.

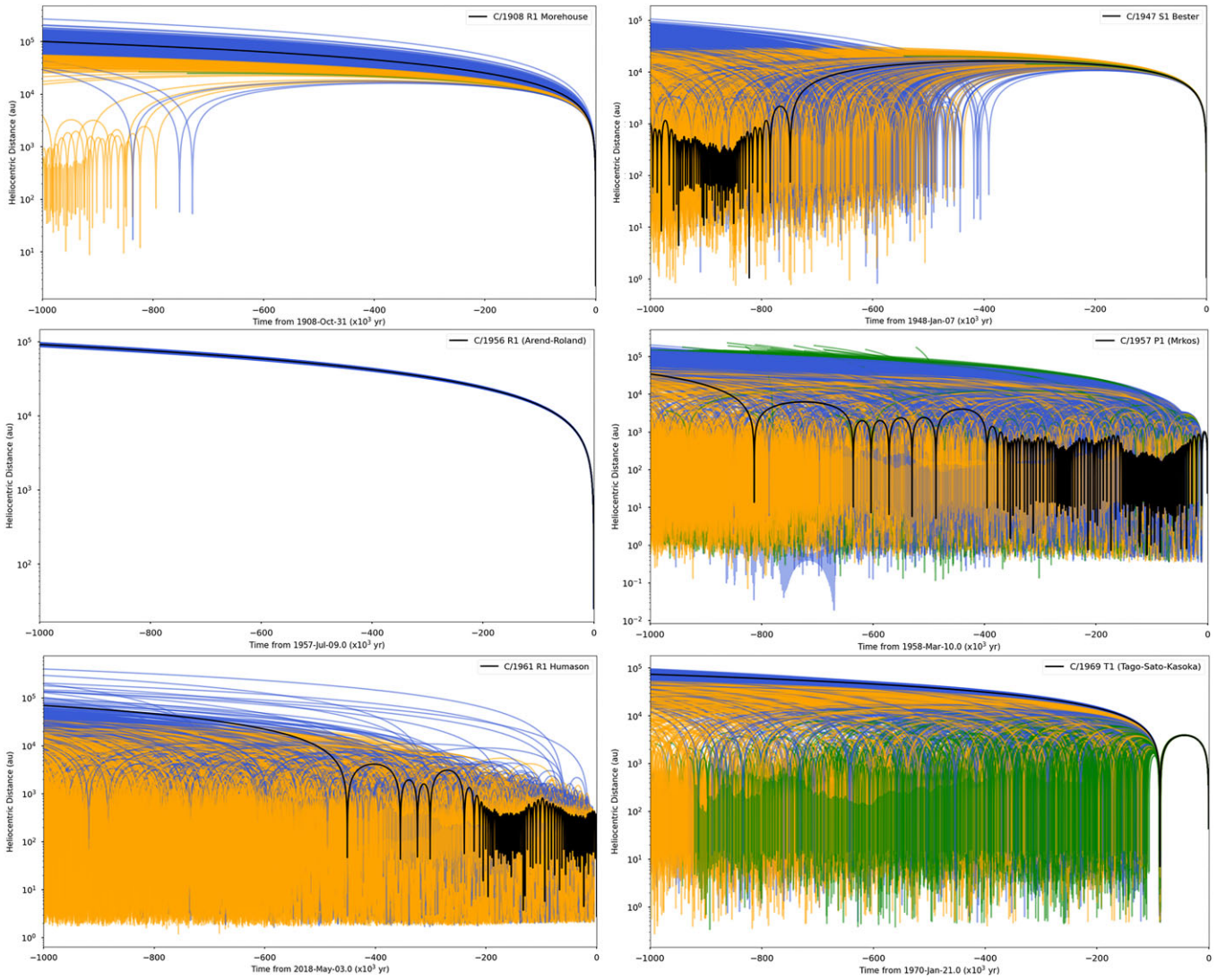

Figure 5. The dynamical history of the first six comets from our sample (black) as estimated with 1000 clones from the MERCURY numerical integrator, from top to bottom, left to right: C/1908 R1 (Morehouse), C/1947 S1 (Bester), C/1956 R1 (Arend–Roland), C/1957 R1 (Mrkos), C/1961 R1 (Humason), and C/1969 T1 ((Tago-Sato-Kosaka). Clones lost to the numerical integrator are shown in green. Those with $e < 1$ at the end of the 1 Myr are shown in orange and those with $e > 1$ are shown in blue.

4.1.2 Dynamical history of C/1908 R1, C/1947 S1, C/1961 R1, C/1987 P1, C/2001 Q4, and C/2002 VQ94

We then proceeded to investigate the dynamical histories of the remaining long-period comets in our sample. The covariance matrices for two comets, C/1940 R2 (Cunningham) and C/1986 P1 (Wilson), were unavailable in the *JPL SBD*. Consequently, we were able to explore the dynamical histories of C/1908 R1 (Morehouse), C/1947 S1 (Bester), C/1956 R1 (Arend–Roland), C/1957 P1 (Mrkos), C/1961 R1 (Humason), C/1969 T1 (Tago-Sato-Kosaka), C/1969 Y1 (Bennett), C/1973 E1 (Kohoutek), C/1975 V1-A, C/1987 P1 (Bradfield), C/2001 Q4 (NEAT), and C/2002 VQ94 (LINEAR). Due to its rapid processing, we used the MERCURY integrator in the same way as we did for Method 1 for comet C/2016 R2. We estimated their dynamical histories to –1 Myr for 1000 clones each. The results are shown in Figs 5 and 6. The statistical results for the final orbital elements are shown in Table 3. Due to the effect of some extreme outlier values, we show the medial value and median absolute deviation of these results, which provide a reliable and robust summary of the central location and dispersion of the orbital element values, allowing for a more accurate characterization of the typical behaviour of the comets in the study. In some cases, clones are lost due to collisions with the planets or between themselves or due to processing errors: these are shown in green. We investigate whether each comet is more likely to be dynamically old (a returning comet) or dynamically new (making its first appearance in the inner Solar System).

(i) Comet C/1908 R1 (Morehouse): despite the limitations of astrometric observations at the time, a discernible dynamical history is evident for Comet C/1908 R1. Only a small fraction (five clones) had previously traversed the inner Solar System within the past 1 Myr, with none approaching within 10 au, and merely three clones originating from distances within 10^4 au of the sun. Remarkably, no encounters with the giant planets were observed, leading to the definitive conclusion that this comet is unequivocally dynamically new, as the probability of an Oort cloud object making two independent journeys to the inner Solar System is exceedingly

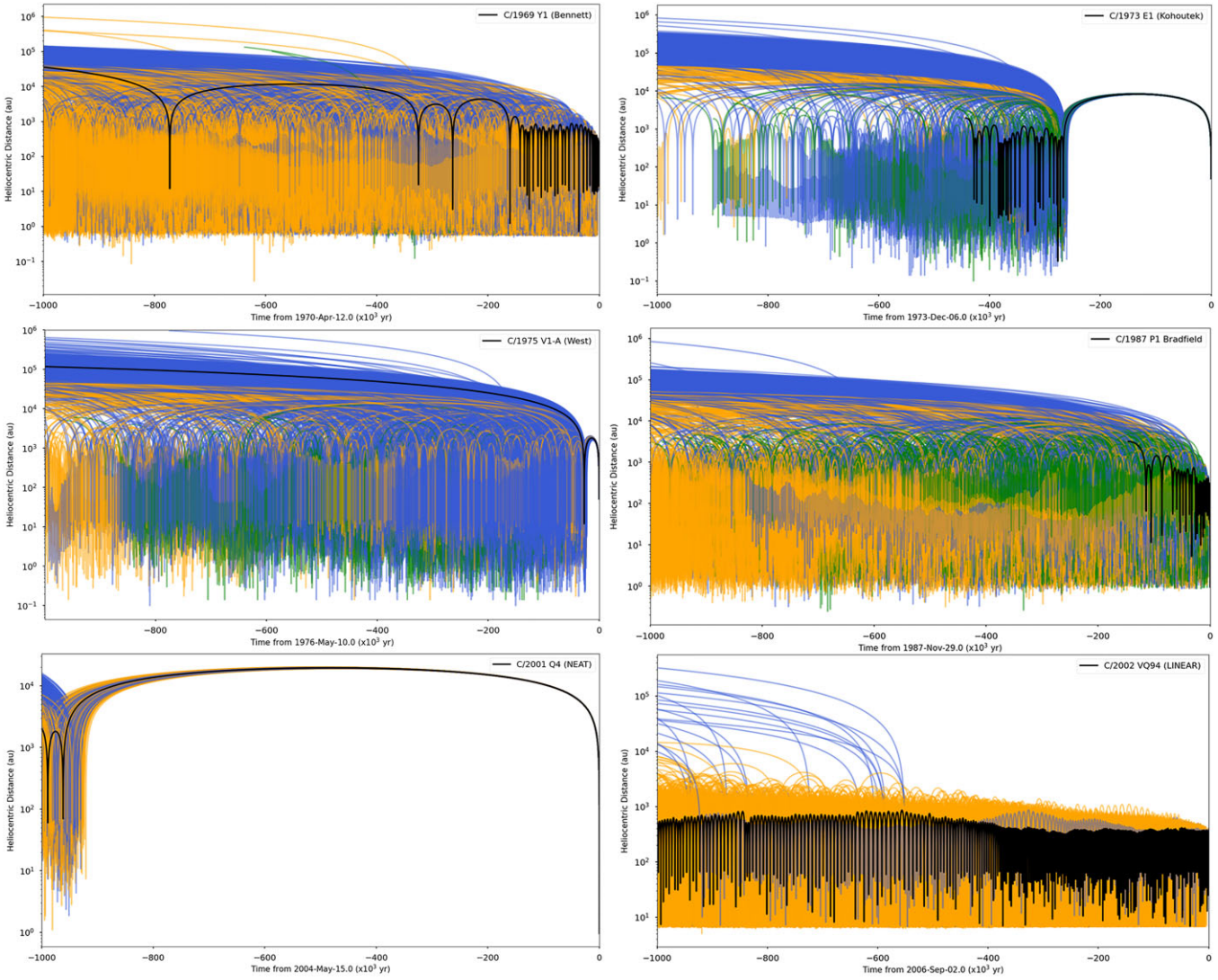

Figure 6. The dynamical history of the last 6 comets from our sample (black) as estimated with 1000 clones from the MERCURY numerical integrator, from top to bottom, left to right: C/1969 Y1 (Benett), C/1973 E1 (Kohoutek), C.1975 V1-A (West), C/1987 P1 (Bradfield), C/2001 Q4 (NEAT), and C/2002 VQ94 (LINEAR). Clones lost to the numerical integrator are shown in green. Those with $e < 1$ at the end of the 1 Myr are shown in orange and those with $e > 1$ are shown in blue.

Table 3. Statistical outcomes and median orbital elements for our clones at the end of the −1 Myr simulation. The uncertainty is expressed as the Median Absolute Deviation (MAD). The dynamical status indicates if the comet is a new visitor to the inner Solar System (New) or if the comet has visited before (Old). The updated N_2/CO ratio is given for comparison.

Comet	$e<1$ (per cent)	$e>1$ (per cent)	Lost (per cent)	r_h (au)	e	Number of orbits >10 au	Dynamical status	N_2/CO
C/1908 R1 (Morehouse)	11.5	88.3	0.2	$(8.32 \pm 1.64) \times 10^4$	1.072 ± 0.062	0 ± 0	New	≥ 0.085
C/1947 S1 (Bester)	44.1	59.9	0.0	$(1.83 \pm 1.46) \times 10^4$	0.999 ± 0.001	0 ± 0	Uncertain	0.071–0.125
C/1956 R1 (Arend–Roland)	0.0	100.0	0.0	$(9.16 \pm 0.12) \times 10^4$	1.129 ± 0.008	0 ± 0	New	>0.125
C/1957 R1 (Mrkos)	34.9	57.5	7.6	$(4.48 \pm 3.86) \times 10^4$	1.020 ± 0.027	12 ± 11	Old	0.028
C/1961 R1 (Humason)	78.4	21.6	0.0	$(1.88 \pm 1.81) \times 10^3$	0.998 ± 0.003	13 ± 9	Old	0.028–0.043
C/1969 T1 (Tago-Sato-Kosaja)	28.0	27.2	44.8	$(4.03 \pm 1.96) \times 10^4$	0.999 ± 0.007	1 ± 1	Old	$\leq$0.043
C/1969 Y1 (Benett)	50.1	49.2	0.7	$(2.14 \pm 2.09) \times 10^4$	0.999 ± 0.006	88 ± 72	Old	0.043
C/1973 E1 (Kohoutek)	5.0	60.8	34.2	$(1.50 \pm 0.61) \times 10^5$	1.783 ± 0.725	1 ± 1	Old	0.100
C/1975 V1-A (West)	12.7	83.6	3.7	$(1.02 \pm 0.45) \times 10^5$	1.125 ± 0.125	2 ± 2	Old	0.011
C/1987 P1 (Bradfield)	31.7	32.9	35.4	$(3.03 \pm 3.01) \times 10^4$	1.000 ± 0.015	103 ± 91	Old	0.028
C/2001 Q4 (NEAT)	54.7	45.3	0.0	$(4.91 \pm 2.60) \times 10^3$	0.999 ± 0.001	0 ± 0	Uncertain	<0.043
C/2002 VQ94 (LINEAR)	98.2	1.8	0.0	$(3.99 \pm 2.21) \times 10^2$	0.978 ± 0.011	21 ± 7	Old	0.085
C/2016 R2 (PanSTARRS)	52.8	42.8	4.4	$(2.67 \pm 2.37) \times 10^4$	0.999 ± 0.003	1 ± 1	Old	0.089

low. The clones exhibit an average eccentricity of 1.16 ± 0.3 at –1 Myr, demonstrating remarkably low dispersion: the absence of any close encounters with the giant planets ensures no outliers are present. Although this alone is insufficient to determine if the comet is of interstellar origin, it does suggest that C/1908 R1 was loosely bound to our Solar System, and would be subject to the interstellar regime, where galactic tidal forces are dominant.

(ii) Comet C/1947 S1 (Bester): the dynamical history of comet C/1947 S1 presents a more nuanced scenario compared to C/1908 R1. At –1 Myr, nearly half (42 per cent) of the generated clones exhibit hyperbolic orbits, while the remaining half (58 per cent) manifests nearly parabolic orbits. Due to the observed mixture of hyperbolic and nearly parabolic orbits, and the lack of passes within the inner Solar System, this comet's dynamical history is uncertain.

(iii) Comet C/1956 R1 (Arend–Roland): this comet exhibits clear characteristics of being dynamically new. At –1 Myr, all of the clones generated display hyperbolic orbits, with an average eccentricity of 1.13 ± 0.01. While it may be tempting to classify this comet as an interstellar visitor, the lack of available information on galactic tides during that time period prevents a definitive determination of whether the comet originated from the Oort cloud. Notably, this conclusion aligns with the findings of Sekanina (1968), who proposed the possibility of it being the 'first interstellar comet known', although they also suggested that extreme non-gravitational forces could account for its characteristics. The similarities in dynamical history with comet C/1908 R1 further underscore the potential loosely bound nature of these comets within our Solar System.

(iv) C/1957 R1 (Mrkos): much like Comet C/1947 S1, the clones are divided nearly in half. These characteristics imply a potential status of being dynamically old, as evidenced by numerous orbits with significant proximity to the sun (a median value of 12 orbits). It also appears this comet may, at one point, have been a periodic comet with an orbit similar to 1P/Halley, though this behaviour is shared by less than half of the clones.

(v) Comet C/1961 R1 (Humason): only 22 per cent of the generated clones displayed a hyperbolic orbit at –1 Myr, indicating a significant majority (78 per cent) of clones being gravitationally bound to the sun. Furthermore, the median number of orbits falling within 10 au is 13. This suggests that Comet C/1961 R1 (Humason) is likely a dynamically old Oort Cloud comet, having made multiple voyages into the Solar System in the past.

(vi) C/1969 T1 (Tago-Sato-Kosaja): similar to C/2016 R2, this comet exhibits a distinct past single orbit; however, the presence of close encounters with the giant planets during its previous revolution leads to a scattering of clones and a loss of nearly half of all clones (448) with extremely eccentric orbits, despite our best efforts and multiple runs. This makes the results frustratingly unreliable. At the end of the simulation, 45 per cent were thus lost, 27 per cent displayed highly eccentric orbits, while the remaining 28 per cent exhibited hyperbolic trajectories. These characteristics suggest that this comet is likely dynamically old, while the loss of clones usually indicates complex close encounters with the giant planets.

(vii) C/1969 Y1 (Benett): we can trace this comet's past back reliably for two orbits. It then exhibits behaviour similar to comets C/1947 S1, C/1956 R1, and C/1961 R1, with a fairly even distribution between hyperbolic (49.2 per cent) and highly eccentric (50.1 per cent) orbits. However, a notable characteristic is the exceptionally high number of orbits: with an average of 270 passes under 10 au, for a median of 88 ± 72 orbits for the generated clones. While its origin is unclear, we can say with confidence that it is dynamically old.

(viii) C/1973 E1 (Kohoutek): in this simulation, we encounter a significant loss of one-third of our clones. However, the results reveal that only 5 per cent of the remaining clones remain bound to the Solar System, while a majority of 61 per cent exhibit a hyperbolic orbit after –1 Myr. With a median final distance of 1.50 ± 0.61 au and an incredibly high median eccentricity of 1.783 ± 0.725, these findings strongly suggest that the comet in question originated from the distant Oort cloud. Despite this origin, the comet still exhibits a confirmed past orbit, indicating it is still dynamically Old.

(ix) C/1975 V1-A (West): much like comets C/1969 T1, C/1973 E1, and R2, its exhibits a single clearly defined orbit. At –1 Myr, there is a 83 per cent likelihood of a hyperbolic orbit while there is a 13 per cent chance of remaining bound to the Solar System. So while it is dynamically old, it has a clear distant Oort cloud origin.

(x) Comet C/1987 P1 (Bradfield): due to heavy numerical losses, it is difficult to be clear about this comet's dynamical past. The remaining clones are split half and half between bound and hyperbolic trajectories. With 353 average passes <10 au per clone, most likely dynamically old. Unfortunately, it has too many numerical losses to be any stronger, more reliable statistics. Our attempts to conduct repeated simulations using multiple batches of randomly generated clones consistently resulted in a loss of a third of the clones, underscoring the chaotic nature of these objects. It became evident that merely increasing the number of clones did not enhance the accuracy of our conclusions when close encounters are involved.

(xi) Comet C/2001 Q4 (NEAT): this appears to be a returning comet, though its last passage at perihelion was over 9×10^5 yr ago. However, due to the fact that it was quite distant in the Oort cloud ($<\sim 10^4$ au), it was subject to the galactic tides and we cannot be entirely sure of its last passage through the inner Solar System, even if there appears to have been one. This is not helped by the 55 per cent/45 per cent split between remaining/hyperbolic comets.

(xii) Comet C/2002 VQ94 (LINEAR): unlike the other comets in this study, C/2002 VQ94 is the only one which remains clearly in our Solar System, with only 18 clones exceeding $e = 1$ at –1 Myr. The eccentricity remains 0.989 on average, slightly lower than most near-parabolic comets, with a median value of 0.978 ± 0.011, the lowest in our sample. On average, each comet makes 25 passes <10 au for a median of 21 ± 7: the rest of time the perihelion remains ∼ 10 au, meaning that while it may not be outgassing each orbit. Its median final distance is $(3.99 \pm 2.21) \times 10^2$, placing its origin much closer than the others, likely from the Kuiper Belt or beyond, perhaps from the scattered disc, as it must have been stored at a high-heliocentric distance in order to keep its volatile content.

It is obvious from these twelve comets that there is no clear dynamical link between their histories. They do not appear to come from a single location in the Oort cloud, though it is likely that they were stored at a large heliocentric distance, in order for them to retain their volatile composition. Of the 13 comets in this study, including R2, only three – C/1908 R1, C/1956 R1, and possibly C/1947 S1 or C/2001 Q4 – can be classified as dynamically new. Interestingly, the first three comets exhibit an incredibly high concentration of N_2, while the latter is moderately N_2-poor. Conversely, certain comets with an extremely high N_2 content, such as C/1973 E1, C/2002 VQ94, and C/2016 R2, are identified as dynamically old. This observation indicates that the N_2 composition of a comet does not bear a direct relationship to its dynamical age. While a more comprehensive analysis of these dynamical histories would indeed be fascinating, the disparate orbital trajectories underline an apparent lack of a definitive connection between N_2 composition and dynamical history.

Table 4. Orbital elements from the CODE catalogue for the previous orbit of each comet, where p indicated the previous passage of the comet in the inner Solar System.

Comet	a_p	Δz (10^{-5} au^{-1})	q_p (au)	Dynamical status	Class	N_2/CO
C/1940 R2 (Cunningham)	31806.62	2.01	2.588	Uncertain	Jumper (KQ)	0.057
C/1947 S1 (Bester)	18811.14	0.017	0.315	Definitely dynamically old	Creeper	0.071–0.125
C/1956 R1 (Arend–Roland)	13007.28	0.089	0.784	Most probably dynamically old	Creeper	0.125
C/1973 E1 (Kohoutek)	54614.96	2.46	42.046	Definitely dynamically new	Jumper (KQ)	0.100
C/1986 P1 (Wilson)	23854.96	0.008	5.12	Most probably dynamically old	Creeper	0.100
C/2001 Q4 (NEAT)	33795.20	0.017	52.036	Definitely dynamically new	Jumper	0.043

4.1.3 Dynamical history of 29P/Schwassmann–Wachmann 1

Much work has been done by others on the subject of 29P's peculiar orbit. Due to its close proximity to Jupiter, 29P's orbit evolves significantly on short time-scales. It would appear 29P's orbit undergoes semimajor axis and eccentricity changes when it comes to a conjunction with Jupiter every ∼50 yr, but these are relatively predictable. (Sarid et al. 2019) estimated that 29P's present-day, very-low-eccentricity orbit (e = 0.043) was established after a 1975 conjunction and will continue until a 2038 Jupiter conjunction nearly doubles its eccentricity and pushes its semimajor axis out to its current aphelion ∼7 au, causing 29P to experience much wider variations in solar heating. They believe it is a new visitor to the Gateway region (Sarid et al. 2019), rather than a return visitor that had spent any significant time in the inner Solar System. This is indicated by its current low-inclination orbit (<10°), high activity at a high heliocentric distance, and the lack of a historical record of a short-period 'super-comet'. Indeed, as its perihelion is at 5.7 au, its volatiles continues to sublimate rapidly. Estimates show this comet had to come to its current orbit from a more stable cometary reservoir, most likely the Oort cloud, with a lower probability of it being from the TNO or Scattered Disc region (Neslušan, Tomko & Ivanova 2017).

4.2 Jumpers and creepers

Kaib & Quinn (2009); Fouchard et al. (2018); Fouchard, Emel'yanenko & Higuchi (2020) searched for a record of the Oort cloud formation process in the orbital distribution of currently observable long-periodic comets. When looking at the previous passage of a comet through the inner Solar System, we can split Oort cloud comets into Jumpers ($q_p > 10$ au) and creepers ($q_p < 10$ au). When the original orbital energy $z = -1/a$ has increased over 10^{-5} au^{-1}over the last orbital period, the comet is called a Kaib–Quinn comet (KQ) (Kaib & Quinn 2009). This splits the comets into four classes: jumpers, KQ-jumpers, creepers, and KQ-creepers. To find the orbital elements of these comets, we use the Warsaw catalogue of cometary orbits, known as the CODE catalogue (Królikowska 2014). This is available on the VizieR data base.[2] as well as on the website[3] As of February 2023, the original orbital elements of 279 comets are available with 1σ uncertainties, including also their previous, current, next, and future orbits, and the values at r = 250 au, which are good indicators for these comets' elements while in the Oort cloud. These values are shown in Table 4 for the comets in our sample included in this catalogue. Of these, we are in agreement when it comes to C/1947 S1 as we both find it is dynamically old. They consider C/2001 Q4 to be dynamically new, while we are uncertain. We disagree for comets C/1956 R1, where we find it to be definitely dynamically new and C/1973 E1 which we find to be dynamically old. In any case, were we to use the Kaib & Quinn (2009); Fouchard et al. (2018); Fouchard et al. (2020) classification of Oort cloud comets, based solely on their semimajor axis a, C/1973 E1, C/1940 R2, and C/2001 Q4 are jumpers, while C/1986 P1, C/1947 S1, and C/1956 R1 would be creepers. Determining if the object is a KQ comet is difficult, as it involves estimating if the object had a close encounter with a planet during its last passage in the inner Solar System. In our dynamical study of C/2016 R2, we find that this comet is a Creeper. Once again, these objects do not have a clear concordant dynamical history.

[2]https://vizier.u-strasbg.fr/
[3]https://pad2.astro.amu.edu.pl/comets/

5 SIMILARITIES WITH PLUTO AND TRITON

Biver et al. (2018) suggest that C/2016 R2 may be a fragment of a differentiated Kuiper belt body in order to explain the large observed hypervolatile abundances. This same theory could be applied to 2I/Borisov as an extra-solar KB object suggested by Cordiner et al. (2020) to explain its CO-rich and H_2O-poor composition. De Sanctis, Capria & Coradini (2001) found that CO and other volatiles could almost be completely absent in the upper layers of a hypothetical bulk differentiated comet: In that case, these two comets could be pieces of the cores of such differentiated comets.

The volatile-rich comets share many similarities with Kuiper Belt bodies Pluto and Triton as all of these bodies have compositions rich in ultravolatiles to some degree. Specifically, the composition of Pluto's Sputnik Planitia is remarkably similar to that of C/2016 R2 and stands out as the one region of Pluto's encounter hemisphere where CO and N_2 ices coexist, though it is mostly N_2-CO ice. The surface of Pluto appears to have an N_2/CO ratio of 250 (or a CO/N_2 ratio of 4×10^{-3} from Glein & Waite (2018). This region has been interpreted as a cold trap where volatile ices have accumulated in a topographic low, possibly originating as an impact basin. The red colour and spectral slope of 'Oumuamua also were a good match to Plutos' surface. However, though similar, the relative abundances of CO, CH_4, and N_2 we observe for C/2016 R2 do not match the surface spectra of Pluto, though the relationship between the surface composition and interior of large KBO has yet to be thoroughly understood (Protopapa et al. 2008), as accretional heating, hydrothermalism, and atmospheric escape are likely to have modified the surface composition after accretion. While C/2016 R2 could have formed from the same solids as those agglomerated by Pluto and Triton, the subsequent evolution and processing of these bodies and the resulting variations in their surface compositions make this analysis difficult.

Along those same lines, a possible explanation for C/2016 R2's composition was presented by Desch & Jackson (2021), who suggest that C/2016 R2 could be a nitrogen iceberg, a fragment of a differentiated KBO surface that was created during the period of

energetic impacts during the 2:1 Jupiter:Saturn resonance epoch. They propose that 1I/'Oumuamua may be an N_2 iceberg chipped off from the surface of an ex-Pluto by an impact during a period of dynamical instability. Since no dust production or outgassing was detected during the passage of Oumuamua, its true composition could not be determined, but the trajectory demanded a non-gravitational force directed away from the sun varying roughly as $1/r^2$, consistent with cometary outgassing, albeit at a slightly higher magnitude than is typical for comets. They found that these unusual properties could be explained if Oumuamua is composed of N_2 ice like that found on the surface of Pluto, suggesting that N_2 ice could provide the non-gravitational acceleration necessary to match observations at either a low albedo ∼0.1, or a high albedo ∼0.64, the latter matching the albedos of the N_2-covered surfaces of outer Solar System bodies like Pluto and Triton. However, recent studies by Levine et al. (2021) have cast doubt on the idea that impacts on extrasolar Kuiper Belt analogs can produce large fragments of N_2 ice, such as Oumuamua. The preservation of intact blocks of N_2 ice during the highly energetic collisions necessary to break apart such objects presents a challenging puzzle to explain. Seligman & Laughlin (2020) find that Oumuamua was more likely composed of H_2 ice, and Bergner & Seligman (2023) suggest that Oumuamua originated as an H2O-rich icy body planetesimal relic broadly similar to Solar System comets. Moreover, Siraj & Loeb (2021) study this theory by examining the mass budget in exo-Pluto planets necessary to produce a population of N_2 icebergs that would explain the detection of Oumuamua and find that stars would have to have a mass of heavy elements exceeding our knowledge of their composition. Only a small fraction of the mass of stars ends in exo-Plutos, making this scenario unlikely. Although the notion that R2 could be a fragment of a differentiated KBO surface presents an intriguing theory, the retention of its N_2 content would present a significant challenge to explain, rendering this scenario less probable. The intriguing nature of N_2-rich comets like C/2016 R2 and their N_2 retention mechanisms warrant further exploration and study in future research.

6 SUMMARY AND DISCUSSION

The fact that there is no shared dynamical history between the comets is significant. There appears to be no link between the N_2/CO ratio and the dynamical history of the comet nor the average number of orbits within the inner Solar System: this would seem to indicate that these objects are not stratified and likely undifferentiated. There does not seem to be a baseline N_2/CO ratio from which these comets would have eroded down with each successive pass near the sun. This would be supported by our observation that the N_2/CO ratio in comet C/2016 R2 varied from day to day (Opitom et al. 2019; Anderson et al. 2022a), though this was in reasonable amounts, and linked to the way the ion tail was sampled. The volatile composition would thus not be linked to the number of passages in the inner Solar System and would indicate that these comets, despite their size, are not differentiated in their bulk composition. Owen & Bar-Nun (1995) point out that as comets are continuously exposed to solar radiation in the inner Solar System, they would be expected to lose any N_2 in their outer layers in a brief period of time: however, these N_2/CO ratios would seem to indicate that no such layers exist and N_2 is present throughout the nucleus of an N_2-rich comet.

The similarity in compositions but distinct dynamical histories of these objects suggests a common origin within a specific region of the Solar System before being ejected to the Oort cloud or scattered disc. Given the limited survival of volatiles after multiple close encounters with the sun since the early formation of the Solar System, it is evident, as supported by previous studies, that comets 1P, 29P, and 67P must have originated as captured objects that remained stored at large heliocentric distances for most of their existence. This prolonged storage allowed them to retain the observed volatile content seen today. Comets C/1908 R1 and C/1956 R1 were clearly stored at the outer edge of the Oort cloud, though further knowledge of the galactic tides must be evaluated in order to determine how stable their position there truly was. They are the only comets for which each clone fits the criteria of dynamically new comets for the entire time of our simulation and thus must be the most pristine. Unfortunately, we cannot determine precisely where in the Oort cloud they were stored for the majority of the Solar System's lifetime. It is also possible that some of our comets could be interstellar in nature, but none had a high enough final eccentricity to be conclusive.

There exists a possibility that our Solar System is rife with volatile-rich comets, but we are simply not observing them. However, since these comets are more productive at higher heliocentric distances, they should be easier to detect, unless there is a process that would prevent N_2 outgassing from being observed: as with the *in situ* measurements of N_2 on 67P's surface, there is perhaps much more N_2 in comets than our spectrometers can observe. Most comets are not bright enough to be observed with high-spectral resolving powers: however, volatile-rich comets are brighter than usual due to their ionic compositions. This should make them more readily discovered and observed with a high spectral resolution, yet their detections are still few and far between. All three H_2O-poor comets have only been discovered in the past decade: One, an interstellar visitor (2I/Borisov); one, enriched in N_2 (C/2016 R2), and one presenting as a usual comet in every other way (C/2009 P1). There may be some selection bias that causes CO-poor comets to be observed more frequently. This could be a result of our modern observational technology: while our spectrometers have higher resolution, they usually require a smaller slit. The first comet tails were observed with photographic plates with a long slit and medium resolution; since the implementation of CCDs ∼ 1990, we have much higher resolution spectroscopy, but the caveat is that spectra have a short slit centered on the nucleus, in the order of arcseconds rather than arcminutes. With UVES short slit, one never sees CO^+ or N_2^+ while still seeing H_2O^+, OH^+ and CH^+. No CO^+ is seen in the centered spectrum of DeVico (Cochran et al. 2000), but it is weakly present in the offset spectrum. However, using long-slit spectroscopy raises the possibility of contamination by atmospheric N_2^+ lines. This compromise may have cost us multiple N_2^+-rich comets.

7 CONCLUSIONS

This study finds no link between the N_2/CO ratio and the dynamical history of N_2-rich comets within the inner Solar System. In addition, N_2-rich comets seem to preserve protosolar N_2/CO values, in contrast to the general observation of comets being depleted in nitrogen compared to protosolar values. Our study re-estimates the N_2/CO ratios of these N_2-rich comets using new N_2 fluorescence factors and finds that they align with the expected values for comets based on estimations of the protosolar nebula. Additionally, the study finds similarities between these comets in terms of their larger-than-usual nucleus size, and rapid variations in tail morphology due to their ionic nature. This indicates that these comets are likely undifferentiated in their bulk composition and that comets would not have their N_2 limited to external layers that would be stripped within a few passes near the sun. These findings suggest that these volatile-rich comets formed in a shared region of the Solar System before being ejected

to the Oort cloud, though further studies are needed to expand on these findings.

The similarities between the composition of C/2016 R2 and Pluto's Sputnik Planitia are intriguing and warrant further study. One possibility is that C/2016 R2 could have formed from the same solids as those agglomerated by Pluto and Triton. Another theory is that C/2016 R2 is a fragment of a differentiated KBO surface that was created during the period of energetic impacts during the 2:1 Jupiter:Saturn resonance epoch. This is supported by its dust-poor composition. The critical difference between these two formation scenarios lies in the timing. If these comets formed from the same primordial grains as Pluto and Triton, or are among the planetesimal leftovers of these two bodies, then they would have had to be stored in the Oort cloud early on so as to survive the sublimation period of the Kuiper Belt (Lisse et al. 2022). This is supported by the dynamical work we did in Anderson et al. (2022b), where we found that planetesimals formed in a particular region of the Protosolar Nebula (∼10 au from the sun) would have been ejected from the Solar System early on, allowing for only a handful to be captured by the Oort cloud, thus explaining the lack of these comets. N_2-rich comets observed today would thus be some of the earliest comets formed in the Solar System and some of the earliest transplants to the Oort cloud. We would need to investigate whether or not N_2-, CO-rich, and H_2O-poor bodies could form naturally from the accumulation of grains or if this composition could only occur in differentiated objects in order to evaluate which scenario is more likely. It would also be interesting to examine the possibility of collisional fragments of differentiated objects being a source of comets: We would need to estimate the likelihood of forming a differentiated KBO, establishing the size of the population; then the odds of collisionally fragmenting this KBO; then the processes which would transport this object to the Oort cloud, or remove them from the Solar System. We would also need to investigate the effect of the collisions themselves on the N_2 and other volatile content. This would be an interesting, long-term project.

Further study is needed to better understand the origin and evolutionary history of these comets. It would be beneficial to study the selection bias in comet observations and to consider using long-slit spectroscopy to potentially detect more N_2-rich comets. Another area of research could be to conduct more *in situ* measurements of N_2 in comets, as there is likely more N_2 present than currently observed by spectroscopes. The spectroscopic study of a comet's coma does not perfectly reflect the composition of the nucleus, as evidenced by the Rosetta mission to 67P. The Rosetta mission has already provided us with a wealth of data and the Comet Interceptor mission has the potential to do the same. The data collected from these missions will not only expand our knowledge of comets and their role in the formation of the Solar System but have the potential to provide us with invaluable information about the origins of our Solar System and the building blocks of life. The unique features of comets, such as their pristine nature, make them ideal targets for study, as they can provide us with a snapshot of the Solar System preserved from the moment of their formation. Additionally, the study of comets can also help us understand the potential for life on other bodies in the Solar System, such as icy moons. *In situ* measurements are key to understanding the composition and distribution of volatiles within cometary nuclei so as to better understand their role in Solar System formation and rebuilding the geography of our protosolar nebula.

8 DATA AVAILABILITY

The data underlying this article will be shared on reasonable request to the corresponding author.

REFERENCES

A'Hearn M. F., Schleicher D. G., Millis R. L., Feldman P. D., Thompson D. T., 1984, AJ, 89, 579

A'Hearn M. F., Millis R. C., Schleicher D. O., Osip D. J., Birch P. V., 1995, Icarus, 118, 223

Anderson S. E., Rousselot P., Noyelles B., Opitom C., Jehin E., Hutsemékers D., Manfroid J., 2022a, MNRAS, 515, 5869

Anderson S. E., Petit J.-M., Noyelles B., Mousis O., Rousselot P., 2022b, A&A, 667, 32

Arpigny C., 1964, PhD thesis, California Institute of Technology

Bar-Nun A., Kleinfeld I., Kochavi E., 1988, Phys. Rev. B, 38, 7749

Bar-Nun A., Notesco G., Owen T., 2007, Icarus, 190, 655

Bergner J., Seligman D., 2023, Nature, 615, 610

Biver N., et al., 2018, A&A, 619, 127

Bockelée-Morvan D., et al., 2000, A&A, 353, 1101

Brandt J. C., Chapman R. D., 2004, Introduction to Comets. Cambridge Univ. Press, Cambridge

Chambers G. F., 1909, The story of the comets simply told for general readers. The Clarendon Press, New York

Chambers J. E., 1999, MNRAS, 304, 793

Chambers J. E., 2012, Mercury: A software package for orbital dynamics, Astrophysics Source Code Library, ascl:1201.008

Christie W., 1908, MNRAS, 69, 47

Cimati A., 1989, Earth Moon Planets, 47, 91

Cochran A. L., Cochran W. D., 2002, Icarus, 157, 297

Cochran A. L., McKay A. J., 2018, ApJ, 854, L10

Cochran A. L., Cochran W. D., Barker E. S., 2000, Icarus, 146, 583

Colina L., Bohlin R. C., Castelli F., 1996, AJ, 112, 307

Cordiner M. A., et al., 2020, Nature Astron., 4, 861

Cremonese G., Fulle M., 1988, A&A, 202, 13

Cruikshank D. P., Roush T. L., Owen T. C., Geballe T. R., de Bergh C., Schmitt B., Brown R. H., Bartholomew M. J., 1993, Sci., 261, 742

de La Baume Pluvinel A., Baldet F., 1911, ApJ, 34, L89

De Sanctis M. C., Capria M. T., Coradini A., 2001, AJ, 121, 2792

Desch S. J., Jackson A. P., 2021, Journal of Geophysical Research (Planets), 126, e06807

Feldman P. D., 2015, ApJ, 812, L115

Feldman P. D., Cochran A. L., Combi M. R., 2004, in Festou M. C., Keller H. U., Weaver H. A.eds, Comets II. University of Arizona Press, Tucson, p. 425

Fernández Y. R., 2002, Earth Moon and Planets, 89, 3

Finson M. L., Probstein R. F., 1968, ApJ, 154, L353

Fouchard M., Higuchi A., Ito T., Maquet L., 2018, A&A, 620, 45

Fouchard M., Emel'yanenko V., Higuchi A., 2020, Celest. Mech. Dyn. Astron., 132, 43

Geiss J., 1987, A&A, 187, 859

Glancy A. E., 1909, PASP, 21, 71

Glein C. R., Waite J. H., 2018, Icarus, 313, 79

Greenstein J. L., 1962, ApJ, 136, L688

Guillaume J., 1908, COMPTES RENDUS DES SÉANCES DE L'ACADÉMIE DES SCIENCES, 147, 833

Huebner W. F., Keady J. J., Lyon S. P., 1992, Ap&SS, 195, 1

Hughes D. W., 2003, MNRAS, 346, 584

Ivanova O. V., Luk'yanyk I. V., Kiselev N. N., Afanasiev V. L., Picazzio E., Cavichia O., de Almeida A. A., Andrievsky S. M., 2016, Planet. Space Sci., 121, 10

Ivanova O. V., Picazzio E., Luk'yanyk I. V., Cavichia O., Andrievsky S. M., 2018, PASS, 157, 34

Jessberger E. K., Kissel J., 1991, in Newburn R. L.J., Neugebauer M., Rahe J.eds, Astrophysics and Space Science Library, Vol. 167, IAU Colloq. 116: Comets in the post-Halley era. Springer, Dordrecht, p. 1075

Kaib N. A., Quinn T., 2009, Science, 325, 1234

Korsun P. P., Ivanova O. V., Afanasiev V. L., 2008, Icarus, 198, 465

Korsun P. P., Rousselot P., Kulyk I. V., Afanasiev V. L., Ivanova O. V., 2014, Icarus, 232, 88

Królikowska M., 2014, A&A, 567, 126
Lamy P. L., Toth I., Fernandez Y. R., Weaver H. A., 2004, The sizes, shapes, albedos, and colours of cometary nuclei. University of Arizona Press, Tucson
Levine W. G., Cabot S. H. C., Seligman D., Laughlin G., 2021, ApJ, 922, L39
Lisse C. M. et al., 2022, PSJ, 3, 112
Lodders K., Palme H., Gail H. P., 2009, Landolt Börnstein, 4B, 712
Lutz B., Womack M., Wagner R., 1993, ApJ, 407, L402
Magnani L., A'Hearn M. F., 1986, ApJ, 302, L477
McKay A. J., et al., 2019, AJ, 158, 128
Merlin F., Lellouch E., Quirico E., Schmitt B., 2018, Icarus, 314, 274
Miles R., 2016, Icarus, 272, 387
Mousis O., Guilbert-Lepoutre A., Lunine J. I., Cochran A. L., Waite J. H., Petit J.-M., Rousselot P., 2012, ApJ, 757, L146
Neslušan L., Tomko D., Ivanova O., 2017, Contributions of the Astronomical Observatory Skalnate Pleso, 47, 7
Noël T., 2018, Cometary Data base, http://www.lesia.obspm.fr/comets/
Ootsubo T., et al., 2012, ApJ, 752, L15
Opitom C., et al., 2019, A&A, 624, 64
Owen T., Bar-Nun A., 1995, Icarus, 116, 215
Owen T. C., et al., 1993, Sci., 261, 745
Pierce D. M., A'Hearn M. F., 2010, ApJ, 718, L340
Protopapa S., Boehnhardt H., Herbst T. M., Cruikshank D. P., Grundy W. M., Merlin F., Olkin C. B., 2008, A&A, 490, 365
Quirico E., Douté S., Schmitt B., de Bergh C., Cruikshank D. P., Owen T. C., Geballe T. R., Roush T. L., 1999, Icarus, 139, 159
Raghuram S., Bhardwaj A., 2012, Planet. Space Sci., 63, 139
Rein H., Liu S. F., 2012, A&A, 537, 128
Rousselot P., Anderson S., Alijah A., Noyelles B., Opitom C., Jehin E., Hutsemékers D., Manfroid J., 2022, A&A, 661, 131
Rubin M. et al., 2015, Science, 348, 232
Rubin M., Engrand C., Snodgrass C., Weissman P., Altwegg K., Busemann H., Morbidelli A., Mumma M., 2020, Space Sci.Rev., 216, 102
Russell H. N., 1916, ApJ, 43, L173
Sarid G., Volk K., Steckloff J. K., Harris W., Womack M., Woodney L. M., 2019, ApJ, 883, L25
Schambeau C. A., Fernández Y. R., Lisse C. M., Samarasinha N., Woodney L. M., 2015, Icarus, 260, 60
Sekanina Z., 1968, Bulletin of the Astronomical Institutes of Czechoslovakia, 19, 343
Seligman D., Laughlin G., 2020, ApJL, 896, L8
Siraj A., Loeb A., 2021, New Astron., 92, 101730
Swings P., 1965, QJRAS, 6, 28
Swings P., Page T., 1950, ApJ, 111, L530
Tichy M. et al., 2002, Minor Planet Electronic Circulars, 2002-V71
van Biesbroeck G., 1962, ApJ, 136, L1155
Warner B., Harding G. A., 1963, The Observatory, 83, 219
Wierzchos K., Womack M., 2018, AJ, 156, 34
Womack M., et al., 2021, Planet. Sci. J., 2, 17
Wyckoff S., Theobald J., 1989, Advances in Space Research, 9, 157
Wyckoff S., Tegler S. C., Engel L., 1991, ApJ, 367, L641

This paper has been typeset from a TEX/LATEX file prepared by the author.